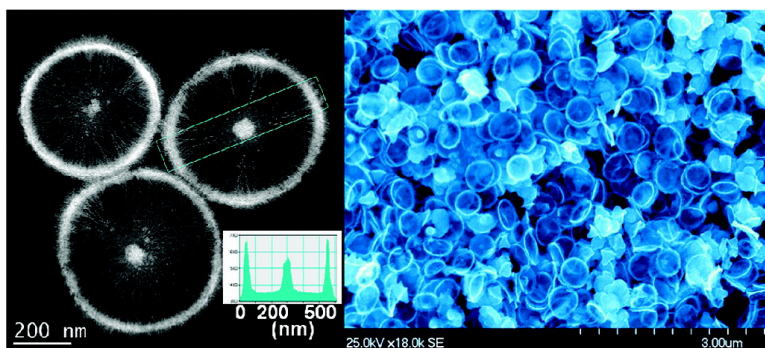


Synthesis of Platinum Nanowheels Using a Bicellar Template

Yujiang Song, Rachel M. Dorin, Robert M. Garcia, Ying-Bing Jiang, Haorong Wang, Peng Li, Yan Qiu, Frank van Swol, James E. Miller, and John A. Shelnett

J. Am. Chem. Soc., **2008**, 130 (38), 12602-12603 • DOI: 10.1021/ja8047464 • Publication Date (Web): 26 August 2008

Downloaded from <http://pubs.acs.org> on February 8, 2009



More About This Article

Additional resources and features associated with this article are available within the HTML version:

- Supporting Information
- Links to the 1 articles that cite this article, as of the time of this article download
- Access to high resolution figures
- Links to articles and content related to this article
- Copyright permission to reproduce figures and/or text from this article

[View the Full Text HTML](#)

Synthesis of Platinum Nanowheels Using a Bicellar Template

Yujiang Song,^{*,†} Rachel M. Dorin,^{†,‡} Robert M. Garcia,^{†,‡} Ying-Bing Jiang,[†] Haorong Wang,^{†,‡}
Peng Li,^{†,||} Yan Qiu,^{†,‡} Frank van Swol,[†] James E. Miller,[†] and John A. Shelnutt^{*,‡,§}

Advanced Materials Laboratory, Sandia National Laboratories, Albuquerque, New Mexico 87106, Department of Chemical and Nuclear Engineering, University of New Mexico, Albuquerque, New Mexico 87131, and Department of Chemistry, University of Georgia, Athens, Georgia 30602

Received June 20, 2008; E-mail: ysong@sandia.gov; jasheln@unm.edu

Disc-like micelles called bicelles are a rare class of microstructures composed of mixed lipid and detergent molecules.¹ Bicelles have also been obtained by self-assembly of two oppositely charged single-chain surfactants or by using a block copolymer.^{2–5} Investigations of bicelles have mainly focused on their alignment and their use as biomimetic membrane models especially for reconstitution of membrane proteins.^{6–10} However, bicelles also provide a unique inhomogeneous reaction environment possessing both low curvature and high curvature regions within a bilayer disk. Although the utilization of bicelles as soft templates for the synthesis of nanomaterials has been suggested,^{2,4} no examples of their successful use for this purpose have been reported. Herein, we show that bicellar templates can be used to control the growth of platinum, producing metal nanodisks and nanowheels.

Bicelles like that illustrated in Figure 1a can be assembled from the surfactants cetyltrimethylammonium bromide (CTAB) and sodium perfluorooctanoate (FC7).^{4,11} Jung and Zasadzinski reported the presence of a small percentage of bicelles mixed with dominant spherical vesicles and cylinders at a CTAB/FC7 molar ratio of 25:75 and 2 wt% total surfactant.⁴ The CTAB/FC7 molar ratio of 50:50 used in this work gives a higher yield of bicelles. For metal growth, platinum was chosen for its dendritic growth characteristics^{12–14} and catalytic activity.^{15,16} Following our previous syntheses of Pt metal nanostructures using lipid vesicles,^{12–14} a typical Pt reduction reaction employed 264 mg of ascorbic acid (AA) as a reducing agent and 10 mL of 20 mM aqueous K₂PtCl₄ added to 10 mL of CTAB (1 mM) and FC7 (1 mM) (0.08 wt% total surfactant); these were allowed to react for at least 1 h at 25 °C to give a black precipitate. A transparent and colorless supernatant was obtained after reduction, suggesting that the reaction was complete. This was confirmed by the absence of UV–visible bands of the Pt(II) complex in the supernatant (Figure S1). Additional details of the synthesis are given in the Supporting Information.

Scanning electron microscopy (SEM) reveals that the black precipitate consists largely of circular platinum nanostructures, along with a small percentage of Pt metal without a defined morphology (Figures 1b, S2). The average diameter of the Pt nanostructures is uniform, 496 ± 55 nm, as determined by the measurement of 100 randomly selected nanostructures (Figure S3). The random packing of the structures results in their being tilted at different angles thus revealing their morphological details. In particular, the tilted circular structure shown in Figure 1c shows the flaring at the edge that produces the wheel-like morphology as well as the thin inner portion of the disk. In Figure 1d,e for a platinum nanowheel lying flat on the supporting substrate, the dendritic sheet features of the inner

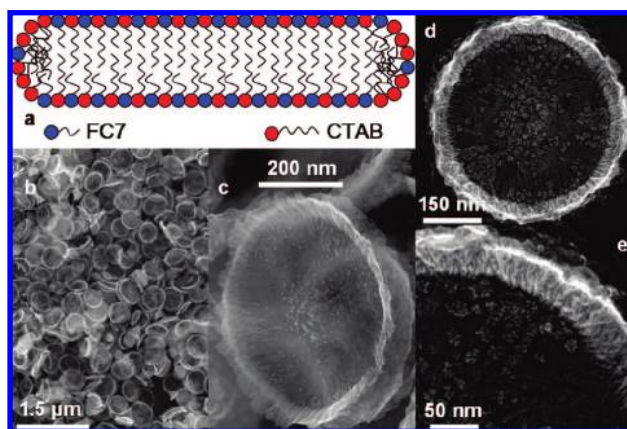


Figure 1. (a) Illustration of the cross-sectional view of a bicelle composed of two different surfactants, CTAB and FC7 in the present system. (b–e) SEM images of platinum nanowheels at different magnifications

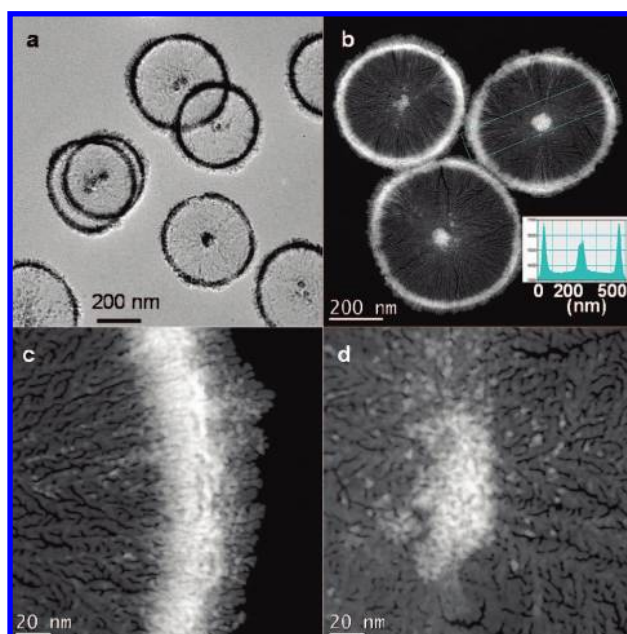


Figure 2. TEM (a) and HAADF STEM (b–d) image of platinum nanowheels (Inset: platinum density profile crossing selected region of a wheel in (b)).

disk are discernible. In these SEM images, very small globular dendrites¹⁴ are also seen growing outward from the dendritic sheet.

The transmission electron microscopy (TEM) images shown in Figure 2 further elucidate the morphology and growth pattern. In particular, the images reveal that the centers of the platinum nanowheels

[†] Sandia National Laboratories.

[‡] University of New Mexico.

[§] University of Georgia.

^{||} Currently at Advanced Technology Development, Intel Corp., Chandler, AZ.

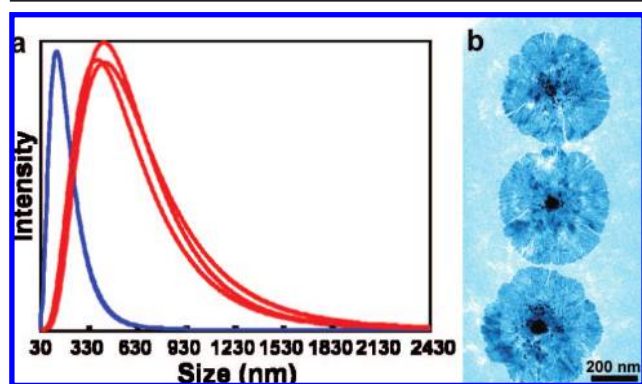


Figure 3. (a) DLS size distributions of bicelles in stock suspension containing 1 mM of CTAB and FC7 (blue), and three repetitions for the reaction system containing bicelles, Pt(II) salt, and AA (0.5 mM CTAB and FC7, 10 mM K_2PtCl_4 , and 150 mM AA (red)). (b) TEM image of platinum nanodisks.

are thickened (Figure 2a). The central thickening is possibly due to the fact that dendritic growth is initiated at a centrally located seed nanoparticle. Slow growth normal to the surface of the sheet occurs throughout the reduction reaction and is thus most extensive near the center of the sheet where growth occurs for the longest time. The reason that the seed particles locate at the center of the bicelle may be due to electrostatic forces caused by the high positive charge density⁴ at the edge of the bicelles. A radial mechanical stress also likely exists in the bicelle because the layers are bound together more tightly at the highly curved edge than at the loose central region, which can thus more easily accommodate the Pt seed particle.

The high-angle annular dark-field scanning TEM (HAADF STEM) images (Figure 2b), for which the brightness is related to the Pt density, confirm that the rim and the center are much more dense than the intermediate region. Additionally, the Pt density profile (Figure 2, inset) indicates that the disk-like part between the center and the edge is roughly uniform in thickness. Consistent with other dendritic Pt sheets formed in lipid bilayers, the thickness is estimated to be about 2 nm.¹³ This can be seen by comparing the size of dendritic tips and the width of bright lines originating from the approximately vertically aligned dendritic branches in the edge region (see Figure S4). In high-magnification images (Figure 2c,d), the dendritic nature of the Pt nanowheels is obvious; the branches are 2–8 nm in width with 1–4 nm spaces between them. The X-ray diffraction pattern of the Pt nanowheels in Figure S5 exhibits characteristic reflection peaks of face-centered cubic Pt, and the peak broadenings are consistent with the nanoscale features seen in the TEM images.

It is likely that flaring occurs when the growing sheet reaches the edge of the templating bicelle. First, confined growth of Pt within the hydrophobic region of the bicellar bilayer¹⁷ gives the same dendritic sheet growth pattern observed previously for liposomal and vesicular bilayers.^{12,13} Second, close examination shows that branching of the inner dendritic sheet occurs from the center outward toward the rim. Moreover, it is likely that crowding occurs and simple sheet growth can no longer be supported when the growing sheet reaches the highly curved edge of the bicelle, leading to the flared edge. So, the diameter of the nanowheel would be determined by the size of the bicelle.

Dynamic light scattering (DLS) results for the stock CTAB/FC7 suspension (pH 6.7) given in Figure 3 (blue line) show that the hydrodynamic size of the bicelles is 144 ± 67 nm. Moreover, the DLS results for the reaction mixture obtained before significant Pt(II) reduction (Figure 3, red line) give a hydrodynamic diameter of 453 ± 216 nm as might be expected for the radically altered

solution conditions of this complex mixture of diluted bicellar solution, Pt salt and aqueous AA, and the different pH (2.7).^{2,18,19} In this mixture, the hydrodynamic size could also be increased by bicellar aggregation and the presence of other mesophases. Nevertheless, a bicellar diameter of 602 nm calculated from the hydrodynamic diameter (details given in the Supporting Information) is compatible with the diameter of the Pt nanowheels obtained from electron microscopy (496 nm), especially given that Pt sheet growth might shrink the bicelles.

To conclusively demonstrate that the flaring at the edge of the Pt nanowheels is a consequence of nanosheet growth reaching the edge of the bicelle, we lowered the Pt(II) concentration from 10 to 5 mM while holding the other parameters constant. For this case, circular dendritic nanodisks with thickened centers are observed, but without the flaring (Figures 3b and S6a). This was expected because the Pt complex is consumed before the sheet reaches the edge of the bicelle. This also provides further proof that the nanowheel grows outward from a central nucleation site.

Finally, when the original synthesis was conducted at 30 and 20 °C, nanowheels with small and large flarings at the edges (Figure S6b,c) were observed, respectively. This is consistent with the production of fewer bicelles containing seed particles at low temperature, leaving more Pt complex per seed and thus more extensive growth for the fewer seeded bicelles. Variation of total surfactant concentration provides additional opportunities to direct the growth of Pt to produce complex nanostructures. The metal growth methods described here might also be used as a means of imaging and discovering structural features of other types of surfactant assemblies and other templating materials.

Acknowledgment. Sandia is a multiprogram laboratory operated by Sandia Corporation, a Lockheed Martin Company, for the U.S. Department of Energy's National Nuclear Security Administration under Contract DEAC04-94AL85000.

Supporting Information Available: Experimental details; UV–vis spectrum; SEM, TEM, and STEM images; size analysis plot; and XRD pattern. This material is available free of charge via the Internet at <http://pubs.acs.org>.

References

- (1) Sanders, C. R.; Landis, G. C. *Biochemistry* **1995**, *34*, 4030.
- (2) Zemb, T.; Dubois, M.; Deme, B.; Gulik-Krzywicki, T. *Science* **1999**, *283*, 816.
- (3) Cui, H. G.; Chen, Z. Y.; Zhong, S.; Wooley, K. L.; Pochan, D. J. *Science* **2007**, *317*, 647.
- (4) Jung, H. T.; Lee, S. Y.; Kaler, E. W.; Coldren, B.; Zasadzinski, J. A. *Proc. Natl. Acad. Sci. U.S.A.* **2002**, *99*, 15318.
- (5) Waggoner, T. A.; Last, J. A.; Kotula, P. G.; Sasaki, D. Y. *J. Am. Chem. Soc.* **2001**, *123*, 496.
- (6) Prosser, R. S.; Evanics, F.; Kitevski, J. L.; Al-Abdul-Wahid, M. S. *Biochemistry* **2006**, *45*, 8453.
- (7) Sanders, C. R.; Oxenoid, K. *Biochim. Biophys. Acta* **2000**, *1508*, 129.
- (8) Sanders, C. R.; Prosser, R. S. *Structure* **1998**, *6*, 1227.
- (9) Marcotte, I.; Auger, M. *Concepts Magn. Reson., Part A* **2005**, *24*, 17.
- (10) Prosser, R. S.; Shiyonovskaya, I. V. *Concepts Magn. Reson.* **2001**, *13*, 19.
- (11) Jung, H. T.; Coldren, B.; Zasadzinski, J. A.; Iampietro, D. J.; Kaler, E. W. *Proc. Natl. Acad. Sci. U.S.A.* **2001**, *98*, 1353.
- (12) Song, Y. J.; Garcia, R. M.; Dorin, R. M.; Wang, H. R.; Qiu, Y.; Shelnutt, J. A. *Angew. Chem., Int. Ed.* **2006**, *45*, 8126.
- (13) Song, Y. J.; Steen, W. A.; Pena, D.; Jiang, Y. B.; Medforth, C. J.; Huo, Q. S.; Pincus, J. L.; Qiu, Y.; Sasaki, D. Y.; Miller, J. E.; Shelnutt, J. A. *Chem. Mater.* **2006**, *18*, 2335.
- (14) Song, Y. J.; Yang, Y.; Medforth, C. J.; Pereira, E.; Singh, A. K.; Xu, H. F.; Jiang, Y. B.; Brinker, C. J.; van Swol, F.; Shelnutt, J. A. *J. Am. Chem. Soc.* **2004**, *126*, 635.
- (15) Antolini, E. *Mater. Chem. Phys.* **2003**, *78*, 563.
- (16) Rolison, D. R. *Science* **2003**, *299*, 1698.
- (17) Garcia, R. M.; Song, Y. J.; Dorin, R. M.; Wang, H. R.; Li, P.; Qiu, Y.; van Swol, F.; Shelnutt, J. A. *Chem. Commun.* **2008**, 2535.
- (18) Nieh, M. P.; Harroun, T. A.; Raghunathan, V. A.; Glinka, C. J.; Katsaras, J. *Biophys. J.* **2004**, *86*, 2615.
- (19) Oberdisse, J.; Porte, G. *Phys. Rev. E* **1997**, *56*, 1965.

JA8047464